LAM, E. J. W., BEURSKENS, P. T. & VAN SMAALEN, S. (1993). *Acta Cryst.* A49, 709–721.

LAM, E. J. W., BEURSKENS, P. T. & VAN SMAALEN, S. (1994). *Acta Cryst.* B50, 690–703.

LEHMAN, M. S. & LARSEN, F. K. (1974). *Acta Cryst.* A30, 580–584.

NORTH, A. C. T., PHILIPS, D. C. & MATHEWS, F. S. (1968). *Acta Cryst.* A24, 351–359.

PAULING, L. (1960). *The Nature of the Chemical Bond*, 3rd ed., pp. 255–256. New York: Cornell Univ. Press.

PETŘÍČEK, V. (1993). *The Computing System JANA93.* Institute of Physics, Academy of Sciences of the Czech Republic, Cukrovarnická 10, 16200 Praha 6, Czech Republic.

PETŘÍČEK, V. & COPPENS, P. (1988). *Acta Cryst.* A44, 235–239.

PETŘÍČEK, V., GAO, Y., LEE, P. & COPPENS, P. (1990). *Phys. Rev. B*, 42, 387–392.

SMAALEN, S. VAN (1992). *Acta Cryst.* A48, 408–410.

SMAALEN, S. VAN (1994). *Crystallogr. Rev.* 4, 79–202.

WOLFF, P. M. DE (1974). *Acta Cryst.* A30, 777–785.

Anion Disorder in the 115–118 K Structures of the Organic Superconductors κ_L-(BEDT-TTF)$_2$Cu(CF$_3$)$_4$(C$_2$H$_3$Cl$_3$) and κ_L-(BEDT-TTF)$_2$Ag(CF$_3$)$_4$(C$_2$H$_3$Cl$_3$) [BEDT-TTF = 3,4;3',4'-Bis(ethylenedithio)-2,2',5,5'-tetrathiafulvalene]

BY URS GEISER, JOHN A. SCHLUETER AND JACK M. WILLIAMS

Chemistry and Materials Science Divisions, Argonne National Laboratory, 9700 South Cass Avenue, Argonne, IL 60439, USA

AND DIETER NAUMANN AND THOMAS ROY

Institut für Anorganische Chemie, Universität Köln, Greinstrasse 6, D-50939 Köln, Germany

Abstract

The low-temperature structures of the isostructural organic superconductors κ_L-(BEDT-TTF)$_2$Cu(CF$_3$)$_4$TCE, 5,5',6,6'-tetrahydro-2,2'-bis{1,3-dithiolo[4,5-b][1,4]dithiin}ylidene tetra(trifluoromethyl)copper trichloroethane (1) (transition temperature, T_c = 4 K), and κ_L-(BEDT-TTF)$_2$Ag(CF$_3$)$_4$TCE, 5,5',6,6'-tetrahydro-2,2'-bis{1,3-dithiolo[4,5-b][1,4]dithiin}ylidene tetra(trifluoromethyl)silver trichloroethane (2) (T_c = 2.6 K), contain crystallographically disordered anions and 1,1,2-trichloroethane (TCE) solvent molecules. Each entity is described as a mirror-symmetric superposition of two asymmetric components. The extent of anion disorder is extraordinary for an organic superconductor. Crystal data: (1) 2C$_{10}$H$_8$S$_8$.CuC$_4$F$_{12}$.C$_2$H$_3$Cl$_3$, M_r = 1242.28, orthorhombic, T = 118 K, a = 12.918 (4), b = 37.899 (7), c = 8.487 (2) Å, V = 4155.1 (18) Å^3, *Pnma* (D_{2h}^{16}, No. 62), Z = 4, $F(000)$ = 2486, D_x = 1.986 Mg m^{-3}, μ(Mo $K\alpha$) = 15.74 cm^{-1}, R = 0.051, wR = 0.039 for 3572 independent reflections with $I > 2\sigma(I)$; (2) 2C$_{10}$H$_8$S$_8$.AgC$_4$F$_{12}$.C$_2$H$_3$Cl$_3$, M_r = 1286.61, orthorhombic, T = 115 K, a = 12.936 (4), b = 37.976 (8), c = 8.526 (2) Å, V = 4188.4 (18) Å^3, *Pnma* (D_{2h}^{16}, No. 62), Z = 4, $F(000)$ = 2553, D_x = 2.040 Mg m^{-3}, μ(Mo $K\alpha$) = 15.16 cm^{-1}, R = 0.050, wR = 0.048 for 4022 independent reflections with $I > 2\sigma(I)$.

1. Introduction

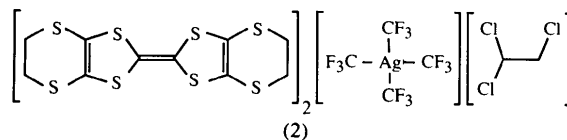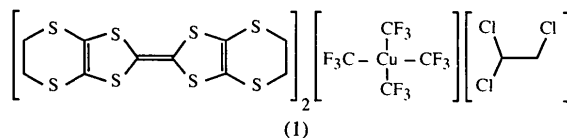Organic superconductors based on the organic electron-donor molecule BEDT-TTF [3,4;3',4'- bis(ethylenedithio)-2,2',5,5'-tetrathiafulvalene, abbreviated ET] now number over 40 (Ishiguro & Yamaji, 1990; Williams, Ferraro, Thorn, Carlson, Geiser, Wang, Kini & Whangbo, 1992), with superconducting transition temperatures (T_c) as high as 12.8 K (at 0.5 kbar pressure) in κ-(ET)$_2$Cu[N(CN)$_2$]Cl (Williams, Kini, Wang, Carlson, Geiser, Montgomery, Pyrka, Watkins, Kommers, Boryschuk, Strieby Crouch, Kwok, Schirber, Overmyer, Jung & Whangbo, 1990). It was recognized many years ago that in cation radical salts, crystallographic disorder in the charge-compensating anion was detrimental to the occurrence of superconductivity. In most cases, superconductivity is totally suppressed by the random electrostatic potentials generated by the disordered anions, *e.g.* in the related salt (TMTSF)$_2$ClO$_4$ (TMTSF = 3,4,3',4'-tetramethyl-2,2',5,5'-tetraselenafulvalene) the noncentrosymmetric anions are disordered on a site with inversion symmetry at room temperature (Bechgaard, Carneiro, Rasmussen, Olsen, Rindorf, Jacobsen, Pedersen & Scott, 1981). Upon slowly lowering the temperature through a first-order crystallographic phase transition at 24 K, the unit cell doubles and the anions form a crystallographically ordered arrangement (Gubser, Fuller, Poehler, Stokes, Cowan, Lee & Bloch, 1982; Pouget, Shirane, Bechgaard & Fabre, 1983). Upon further cooling, the salt becomes superconducting at 1.4 K (Bechgaard, Carneiro, Olsen, Rasmussen & Jacobsen, 1981). However, if the cooling is carried out too rapidly, the phase transition is suppressed and the metastable room-temperature structure is locked in at low temperature (Pouget,

Shirane, Bechgaard & Fabre, 1983). Under those circumstances, superconductivity is not observed. Similarly, in the isostructural series (space group $P\bar{1}$, $Z = 1$) of salts β-$(ET)_2X$, where X is a linear triatomic anion located on an inversion center, the salts with centrosymmetric anions, i.e. I_3^-, IBr_2^- and AuI_2^-, are all superconductors, whereas the salt with the noncentrosymmetric I_2Br^- anion remains in the normal state [see Williams, Ferraro, Thorn, Carlson, Geiser, Wang, Kini & Whangbo (1992) for references]. In β-$(ET)_2I_3$, cooled under ambient pressure, an incommensurate displacive modulation appears below 175 K, and T_c is 1.5 K. If the cooling is carried out under a modest pressure of less than 1×10^5 kPa, the structure remains commensurate (Schultz, Wang, Williams & Filhol, 1986), and $T_c = 7$–8 K, in excellent agreement with the correlation between anion length and T_c derived from the other β-phase salts which do not exhibit the transition to a modulated structure. In the case of the isostructural series κ-$(ET)_2Cu[N(CN)_2]X$ (X = Cl, Br, I), the former two members are superconductors with $T_c = 12.8$ (at 0.5×10^5 kPa; the highest T_c reported for any organic superconductor excluding fullerenes; Williams, Kini, Wang, Carlson, Geiser, Montgomery, Pyrka, Watkins, Kommers, Boryschuk, Strieby Crouch, Kwok, Schirber, Overmyer, Jung & Whangbo, 1990) and 11.8 K (the highest T_c at ambient pressure; Kini, Geiser, Wang, Carlson, Williams, Kwok, Vandervoort, Thompson, Stupka, Jung & Whangbo, 1990). On the other hand, the iodide analog is not a superconductor even under pressure (Geiser, Schultz, Wang, Watkins, Stupka, Williams, Schirber, Overmyer, Jung, Novoa & Whangbo, 1991). Apart from the slightly larger unit cell compared with chloro and bromo salts, the only structural difference found at low temperature, was conformational disorder in one of the ethylene end-groups of the donor molecule. Thus, disorder on either the anion or the electron-donor molecule can be detrimental to superconductivity in these systems.

We have recently discovered a new ET-based organic superconductor, viz. κ_L-$(ET)_2Cu(CF_3)_4$ (TCE), with $T_c = 4$ K (Schlueter, Geiser, Williams, Wang, Kwok, Fendrich, Carlson, Achenbach, Dudek, Naumann, Roy, Schirber & Bayless, 1994).* The room-temperature structure of this material was briefly described in the initial report. At 298 K it was found that both the $Cu(CF_3)_4^-$ anion and the TCE solvent molecule were crystallographically disordered. Since it is highly unusual to find such disorder in organic superconductors (vide supra), we determined the structure at 118 K with the expectation that the disorder would be reduced or

---

* The subscript 'L' denotes the phase with the lower T_c in the ET:Cu(CF$_3$)$_4$:TCE system. Another distinct phase κ_H with $T_c = 9$ K has also been reported by Schlueter, Carlson, Williams, Geiser, Wang, Welp, Kwok, Fendrich, Dudek, Achenbach, Naumann, Roy, Schirber & Bayless (1994).

absent at the lower temperature. In this paper, we report that the anion and solvent molecule disorder are still present at 118 K, and we are able to fully describe the disorder model in terms of two overlapping orientations of the components. Due to higher thermal motion at room temperature, we were not able to fully resolve such a model in the initial report.

Subsequently, we discovered that the analogous $Ag(CF_3)_4^-$ salt was also a superconductor (Schlueter, Carlson, Geiser, Wang, Williams, Kwok, Fendrich, Welp, Keane, Dudek, Komosa, Naumann, Roy, Schirber, Bayless & Dodrill, 1994). At room temperature, only a set of lattice parameters was obtained. An intensity data collection was aborted after only 2 d because the crystal lost solvent, and the crystal lattice collapsed. Therefore, we concentrated on a structural study at a lower temperature where no solvent loss occurred. The results of this study are presented in this paper.

$$\left[\left(\begin{array}{c}S\\S\end{array}\!\!\!\!>\!\!=\!\!<\!\!\!\!\begin{array}{c}S\\S\end{array}\right)\!\!\!\left(\begin{array}{c}S\\S\end{array}\!\!\!\!>\!\!=\!\!<\!\!\!\!\begin{array}{c}S\\S\end{array}\right)\right]_2 \left[\begin{array}{c}CF_3\\F_3C-\overset{|}{\underset{|}{Cu}}-CF_3\\CF_3\end{array}\right]\left[\begin{array}{c}Cl\quad Cl\\ \diagdown\!\!\diagup \\ Cl\end{array}\right]$$

(1)

$$\left[\left(\begin{array}{c}S\\S\end{array}\!\!\!\!>\!\!=\!\!<\!\!\!\!\begin{array}{c}S\\S\end{array}\right)\!\!\!\left(\begin{array}{c}S\\S\end{array}\!\!\!\!>\!\!=\!\!<\!\!\!\!\begin{array}{c}S\\S\end{array}\right)\right]_2 \left[\begin{array}{c}CF_3\\F_3C-\overset{|}{\underset{|}{Ag}}-CF_3\\CF_3\end{array}\right]\left[\begin{array}{c}Cl\quad Cl\\ \diagdown\!\!\diagup \\ Cl\end{array}\right]$$

(2)

2. Experimental

2.1. Structure of κ_L-$(ET)_2Cu(CF_3)_4$(TCE)

Black crystals of κ_L-$(ET)_2Cu(CF_3)_4$(TCE) (1) with a distorted hexagonal plate shape were grown electrochemically, as previously reported (Schlueter, Geiser, Williams, Wang, Kwok, Fendrich, Carlson, Achenbach, Dudek, Naumann, Roy, Schirber & Bayless, 1994). The addition of 10% ethanol to the TCE solvent resulted in thicker, but overall smaller crystals compared with pure TCE. One such crystal (size $0.34 \times 0.25 \times 0.15$ mm) with well developed (101), (100) and (010) (plate plane) faces was mounted on a Syntex $P2_1$ four-circle diffractometer (Mo radiation with graphite monochromator, $\lambda = 0.7107$ Å, diffractometer controlled by a Crysta-Logic computer interface system) and cooled to 118 K in a nitrogen gas stream. The unit cell was determined from the setting angles of 34 carefully centered reflections with $21 < 2\theta < 33°$. The intensities of 6628 reflections were collected in the ω-scan mode ($1.2°$ ω width, 1.5–6 min^{-1}, $4 \le 2\theta \le 56°$, $0.049 \le \sin\theta/\lambda \le 0.661$, $-1 \le h \le 17$, $-1 \le k \le 50$, $0 \le l \le 11$, three standards every 58 reflections, random variations < 2%), which resulted in 5092 unique (merging $R = 0.028$) allowed reflections. The data were corrected for Lorentz and polarization effects, and an absorption correction (integra-

tion method) based on the measured crystal shape was applied ($T_{min} = 0.706$, $T_{max} = 0.800$). The computer programs used were part of the *UCLA Crystallographic Program Package* (Strouse, 1985). The statistical weight assigned *a priori* to each observation was $\sigma^{-2}(F_o)$, where $\sigma(F_o)$ was derived from $\sigma(I)$, based on counting statistics and an 'instability factor' of 0.02.

Starting coordinates for the ET donor molecule C and S atoms, the anion Cu atom, and the solvent Cl atoms were obtained from the room-temperature structure (Schlueter, Geiser, Williams, Wang, Kwok, Fendrich, Carlson, Achenbach, Dudek, Naumann, Roy, Schirber & Bayless, 1994). Subsequent difference-Fourier maps revealed the trifluoromethyl C atoms (atoms C11A and C11B were treated as one atom at that stage) and several peaks compatible with fluorine atomic positions. Preliminary anisotropic refinement with variable occupancies of the F atoms converged to a model, where each trifluoromethyl group contained four F positions in a rhombus-like arrangement. In each case the two F atoms, which were furthest apart (F13A and F13B on one group, F23A and F23B on the other), refined with occupancies of ca 0.5, whereas the other two atoms refined with approximately unit occupancies and extremely anisotropic thermal parameters. The thermal ellipsoid of C11 was also very much elongated. At this stage, it was recognized that each CF$_3$ group was better modeled with a superposition of two half-occupied groups rotated by 180° with respect to each other. In one case (C11A and B), better agreement factors and near-isotropic thermal parameters were obtained using two half-occupied C-atom positions. No such splitting was necessary for the C12 position.

For the solvent molecule, two superimposed half-occupied (by symmetry) orientations of the central C—C ethane backbone were found. An isosceles triangle of Cl atoms (two atoms related by mirror symmetry) accommodates both orientations without the need for split Cl positions. For the final full-matrix least-squares refinement, fixed H-atom positions were calculated ($d_{C—H} = 0.95$ Å,* $U_{iso} = 0.0253$ Å^2) for both the ET molecule and TCE solvent molecule. All non-H atoms were refined with anisotropic thermal parameters. Convergence was reached with agreement factors $R = 0.051$, $wR = 0.039$, and goodness-of-fit = 1.38 for 3572 observations with $I > 2\sigma(I)$ and 337 varied parameters. The maximal features on a difference-Fourier map were +0.7 and 0.7 e Å^{-3} in the vicinity of S2 and Cu, respectively. A trial refinement in the noncentrosymmetric space group $Pn2_1a$ was not successful: large correlations between mirror-related (in *Pnma*) atomic parameters prevented convergence

and led to nonpositive thermal parameters, while no improvement in agreement factors was obtained. Therefore, the space group *Pnma* was confirmed, in agreement with intensity statistics.*

2.2. Structure of κ_L-(ET)$_2$Ag(CF$_3$)$_4$(TCE)

κ_L-(ET)$_2$Ag(CF$_3$)$_4$(TCE) (2) was prepared as described by Schlueter, Carlson, Geiser, Wang, Williams, Kwok, Fendrich, Welp, Keane, Dudek, Komosa, Naumann, Roy, Schirber, Bayless & Dodrill (1994). All crystals were stored in a freezer over dry ice until used. One such black shiny crystal (size $0.50 \times 0.28 \times 0.08$ mm) was mounted on the same diffractometer system as (1). At room temperature, an orthorhombic unit cell of $a = 13.175$ (2), $b = 38.174$ (3), $c = 8.5951$ (10) Å, $V = 4322.8$ (8) Å^3 was determined from the setting angles of 40 centered reflections with $21 < 2\theta < 33°$, and the crystal was then cooled to 115 K. At that temperature, the unit cell shrank to $a = 12.936$ (4), $b = 37.976$ (8), $c = 8.526$ (2) Å, $V = 4188.4$ (18) Å^3. These lattice parameters and a similar distribution of intense reflections indicated that the structures of (1) and (2) were probably very similar. With the same scan parameters as in (1), 6619 intensity data were collected within the limits $4 \le 2\theta \le 55°$, $0.049 \le \sin\theta/\lambda \le 0.650°$, $0 \le h \le 16$, $-1 \le k \le 49$, $-1 \le l \le 11$. The data were processed analogously to (1), with $T_{min} = 0.539$, $T_{max} = 0.892$ and 4877 unique (merging $R = 0.021$) allowed reflections.

For the refinement, starting coordinates from (1) were used in space group *Pnma*. The refinement proceeded smoothly (the largest shifts were due to the increased metal-to-carbon bond length in 2), again requiring a split C11 atom. Since the distance between the two C11 positions was slightly smaller than in (1), the anisotropic thermal parameters of C11B were constrained to be equal to those of C11A, in order to avoid large correlations. H-atom positions were calculated as in (1). Convergence was obtained at $R = 0.050$, $wR = 0.048$ and goodness-of-fit = 2.33 [this somewhat large value is probably due to minor short-term fluctuations in the detector electronics, resulting in a slight underestimation of the $\sigma(I)$ values] for 4022 observations with $I > 2\sigma(I)$ and 331 varied parameters. The maximal features on a difference-Fourier map were +2.5 and 1.1 e Å^{-3}, both in the vicinity of the Ag atom.

3. Results and discussion

Coordinates and equivalent isotropic thermal parameters are given in Tables 1 and 2, whereas bond lengths and angles are listed in Tables 3 and 4 for the Cu- and

---

* The distance of 0.95 Å from the C-atom position is typical for the maximum in H-atom electron density. For geometry calculation, H-atom positions were also calculated at the internuclear distance of 1.09 Å in order to facilitate comparisons with future neutron diffraction studies.

Table 1. *Fractional atomic coordinates, equivalent isotropic thermal parameters (Å^2) and site occupancies (other than those required by site symmetry) in κ_L-$(ET)_2Cu(CF_3)_4(TCE)$*

$$U_{eq} = (1/3) \sum_i \sum_j U_{ij} a_i^* a_j^* \mathbf{a}_i.\mathbf{a}_j.$$

	x	y	z	U_{eq}	Occupancy
S1	0.38001 (8)	0.05013 (3)	0.27170 (13)	0.0187 (3)	1.0
S2	0.24910 (9)	0.02164 (3)	0.01774 (12)	0.0178 (3)	1.0
S3	0.52394 (9)	−0.01622 (3)	0.26723 (13)	0.0193 (3)	1.0
S4	0.39830 (8)	−0.05002 (3)	0.01966 (12)	0.0173 (3)	1.0
S5	0.25874 (9)	0.11523 (3)	0.31932 (13)	0.0210 (3)	1.0
S6	0.10573 (9)	0.08180 (3)	0.00714 (14)	0.0237 (3)	1.0
S7	0.65549 (9)	−0.07736 (3)	0.33018 (13)	0.0230 (3)	1.0
S8	0.50313 (11)	−0.11907 (3)	0.03945 (14)	0.0306 (4)	1.0
C1	0.3559 (3)	0.01573 (10)	0.1409 (5)	0.0146 (11)	1.0
C2	0.4176 (3)	−0.01344 (10)	0.1402 (5)	0.0152 (12)	1.0
C3	0.2731 (3)	0.07574 (10)	0.2145 (5)	0.0153 (11)	1.0
C4	0.2142 (3)	0.06289 (11)	0.0973 (5)	0.0160 (12)	1.0
C5	0.5536 (3)	−0.06002 (10)	0.2200 (5)	0.0170 (12)	1.0
C6	0.4959 (3)	−0.07553 (11)	0.1074 (5)	0.0174 (12)	1.0
C7	0.1795 (4)	0.13965 (11)	0.1822 (5)	0.0271 (14)	1.0
C8	0.0824 (4)	0.12006 (12)	0.1306 (5)	0.0270 (15)	1.0
C9	0.6780 (4)	−0.11876 (12)	0.2302 (6)	0.0298 (15)	1.0
C10	0.5802 (4)	−0.13886 (11)	0.1930 (5)	0.0282 (15)	1.0
Cu	0.18577 (6)	0.2500	0.71055 (8)	0.0173 (2)	1.0
C11A	0.2517 (14)	0.2184 (5)	0.561 (2)	0.031 (5)	0.5
F11A	0.2974 (13)	0.1908 (4)	0.6326 (12)	0.045 (4)	0.5
F12A	0.1861 (10)	0.2047 (2)	0.4545 (14)	0.055 (4)	0.5
F13A	0.3293 (5)	0.2326 (2)	0.4795 (7)	0.051 (2)	0.5
C11B	0.2123 (13)	0.2100 (4)	0.564 (2)	0.024 (5)	0.5
F11B	0.3086 (12)	0.1963 (4)	0.5707 (11)	0.036 (3)	0.5
F12B	0.1973 (10)	0.2191 (2)	0.4087 (11)	0.036 (3)	0.5
F13B	0.1479 (5)	0.18160 (14)	0.5790 (7)	0.037 (2)	0.5
C12	0.1434 (4)	0.21352 (14)	0.8601 (7)	0.036 (2)	1.0
F21A	0.2108 (6)	0.2027 (2)	0.9536 (10)	0.055 (3)	0.5
F22A	0.0504 (8)	0.2194 (2)	0.9230 (10)	0.043 (3)	0.5
F23A	0.1172 (5)	0.18196 (14)	0.7666 (9)	0.050 (2)	0.5
F21B	0.2077 (6)	0.1850 (2)	0.8725 (8)	0.042 (3)	0.5
F22B	0.0500 (7)	0.2032 (2)	0.8732 (10)	0.039 (3)	0.5
F23B	0.1629 (5)	0.2262 (2)	1.0268 (6)	0.035 (2)	0.5
Cl1	0.4280 (2)	0.2500	−0.0884 (6)	0.0348 (6)	1.0
Cl2	0.43451 (12)	0.19333 (3)	0.1804 (2)	0.0453 (5)	1.0
Cl3	0.4051 (7)	0.2592 (2)	0.1165 (9)	0.024 (3)	0.5
Cl4	0.4750 (7)	0.2370 (2)	0.2171 (10)	0.024 (3)	0.5

Table 2. *Fractional atomic coordinates, equivalent isotropic thermal parameters (Å^2) and site occupancies (other than those required by site symmetry) in κ_L-$(ET)_2Ag(CF_3)_4(TCE)$*

$$U_{eq} = (1/3) \sum_i \sum_j U_{ij} a_i^* a_j^* \mathbf{a}_i.\mathbf{a}_j.$$

	x	y	z	U_{eq}	Occupancy
S1	0.37967 (9)	0.05008 (3)	0.26986 (14)	0.0180 (3)	1.0
S2	0.24928 (9)	0.02102 (3)	0.01817 (13)	0.0171 (3)	1.0
S3	0.52472 (9)	−0.01584 (3)	0.26571 (14)	0.0187 (3)	1.0
S4	0.39965 (9)	−0.05013 (3)	0.02092 (13)	0.0169 (3)	1.0
S5	0.25653 (10)	0.11444 (3)	0.31868 (14)	0.0196 (3)	1.0
S6	0.10374 (10)	0.08034 (3)	0.00941 (14)	0.0224 (3)	1.0
S7	0.65602 (10)	−0.07673 (3)	0.33125 (14)	0.0234 (4)	1.0
S8	0.50438 (12)	−0.11895 (3)	0.0429 (2)	0.0300 (4)	1.0
C1	0.3560 (4)	0.01540 (11)	0.1409 (5)	0.0150 (12)	1.0
C2	0.4182 (3)	−0.01352 (12)	0.1407 (5)	0.0150 (12)	1.0
C3	0.2721 (4)	0.07495 (11)	0.2148 (5)	0.0164 (12)	1.0
C4	0.2130 (3)	0.06196 (12)	0.0979 (5)	0.0164 (13)	1.0
C5	0.5539 (4)	−0.05980 (11)	0.2216 (5)	0.0165 (13)	1.0
C6	0.4968 (4)	−0.07535 (12)	0.1093 (5)	0.0170 (13)	1.0
C7	0.1768 (4)	0.13852 (12)	0.1817 (5)	0.0238 (14)	1.0
C8	0.0805 (4)	0.11865 (13)	0.1319 (6)	0.0252 (15)	1.0
C9	0.6809 (4)	−0.11758 (13)	0.2290 (7)	0.030 (2)	1.0
C10	0.5839 (4)	−0.13845 (13)	0.1941 (6)	0.028 (2)	1.0
Ag	0.18359 (4)	0.2500	0.70721 (6)	0.0143 (1)	1.0
C11A	0.245 (2)	0.2140 (9)	0.548 (5)	0.021 (5)	0.5
F11A	0.2872 (12)	0.1874 (4)	0.607 (2)	0.088 (6)	0.5
F12A	0.179 (2)	0.2025 (6)	0.446 (3)	0.0186 (13)	0.5
F13A	0.3200 (12)	0.2266 (2)	0.464 (2)	0.0125 (6)	0.5
C11B	0.215 (2)	0.2087 (9)	0.549 (5)	0.021	0.5
F11B	0.3169 (8)	0.1966 (4)	0.5660 (13)	0.050 (4)	0.5
F12B	0.2077 (13)	0.2167 (3)	0.3977 (10)	0.039 (3)	0.5
F13B	0.1615 (7)	0.1799 (2)	0.5612 (9)	0.038 (3)	0.5
C12	0.1403 (4)	0.21133 (14)	0.8695 (6)	0.027 (2)	1.0
F21A	0.2100 (8)	0.2049 (3)	0.977 (2)	0.079 (5)	0.5
F22A	0.0511 (10)	0.2166 (3)	0.934 (2)	0.061 (5)	0.5
F23A	0.1260 (7)	0.1784 (2)	0.7996 (12)	0.053 (3)	0.5
F21B	0.1955 (10)	0.1820 (2)	0.8690 (10)	0.061 (4)	0.5
F22B	0.0429 (9)	0.2016 (3)	0.874 (2)	0.072 (5)	0.5
F23B	0.1550 (7)	0.2222 (2)	1.0252 (8)	0.040 (3)	0.5
Cl1	0.4260 (2)	0.2500	−0.0899 (2)	0.0352 (6)	1.0
Cl2	0.43430 (13)	0.19345 (4)	0.1762 (2)	0.0469 (5)	1.0
Cl3	0.4027 (7)	0.2592 (2)	0.1166 (11)	0.023 (3)	0.5
Cl4	0.4718 (8)	0.2371 (2)	0.2160 (12)	0.025 (3)	0.5

Ag-containing salts, respectively. Their structures are essentially the same, except for the effects attributable to the increased metal-to-carbon bond length in the Ag-containing salt. They each contain alternating layers of positively charged ET electron-donor molecules and layers composed of the anions and solvent molecules. The contents of a unit cell and surroundings are shown in Fig. 1. Two layers of each occur per unit cell repeat along the layer normal (b axis).

Fig. 2 shows a labeled top and side view of the ET molecule as it occurs in salt (1), and it is indistinguishable from the corresponding view in (2). Almost all corresponding bond distances and angles are the same within less than 1 e.s.d., and all are within 2 e.s.d.'s from each other. As is normally the case in these salts, the central portion of the molecule comprising the inner six C atoms and the S atoms is essentially planar. The average C—S distance for the inner six C atoms is 1.75 (1) Å, and the central C=C double-bond distance is 1.363 (6) for (1) or 1.361 (6) Å for

(2), in excellent agreement with published values for ET molecules with the average charge $+\frac{1}{2}$ (Williams, Wang, Emge, Geiser, Beno, Leung, Carlson, Thorn, Schultz & Whangbo, 1987). The lengths of these bonds have been found to be sensitive indicators of the charge
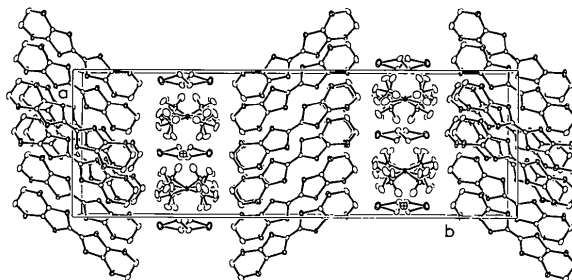

Fig. 1. Perspective view of the unit cell of κ_L-$(ET)_2Cu(CF_3)_4(TCE)$, projected into the ab plane. H atoms are omitted for clarity and thermal ellipsoids are drawn at the 50% probability level.

Table 3. *Geometric parameters* (Å, °) *in* κ_L-(ET)$_2$Cu(CF$_3$)$_4$(TCE)

S1—C1	1.740 (4)	C9—C10	1.509 (7)
S1—C3	1.756 (4)	Cu—C11A	1.94 (2)
S2—C1	1.745 (4)	Cu—C11B	1.99 (2)
S2—C4	1.761 (4)	Cu—C12	1.955 (5)
S3—C2	1.750 (4)	C11A—F11A	1.35 (2)
S3—C5	1.750 (4)	C11A—F12A	1.34 (2)
S4—C2	1.741 (4)	C11A—F13A	1.33 (2)
S4—C6	1.755 (4)	C11B—F11B	1.35 (2)
S5—C3	1.751 (4)	C11B—F12B	1.38 (2)
S5—C7	1.805 (4)	C11B—F13B	1.37 (2)
S6—C4	1.750 (4)	C12—F21A	1.247 (8)
S6—C8	1.814 (5)	C12—F22A	1.334 (11)
S7—C5	1.743 (4)	C12—F23A	1.474 (8)
S7—C9	1.807 (4)	C12—F21B	1.368 (8)
S8—C6	1.751 (4)	C12—F22B	1.273 (10)
S8—C10	1.803 (5)	C12—F23B	1.515 (8)
C1—C2	1.363 (6)	C13—C14	1.500 (11)
C3—C4	1.344 (6)	C13—Cl1	1.799 (8)
C5—C6	1.347 (6)	C13—Cl2^i	1.918 (8)
C7—C8	1.522 (7)	C14—Cl2	1.764 (8)
C1—S1—C3	95.6 (2)	C11A—Cu—C12^i	169.5 (5)
C1—S2—C4	95.0 (2)	C11B—Cu—C12	85.1 (5)
C2—S3—C5	95.0 (2)	C11B—Cu—C12^i	172.9 (5)
C2—S4—C6	95.0 (2)	C12—Cu—C12^i	90.0 (3)
C3—S5—C7	99.8 (2)	F11A—C11A—F12A	106.3 (15)
C4—S6—C8	102.0 (2)	F11A—C11A—F13A	102.6 (15)
C5—S7—C9	101.4 (2)	F11A—C11A—Cu	111.9 (13)
C6—S8—C10	100.6 (2)	F12A—C11A—F13A	106.6 (15)
C2—C1—S1	120.4 (3)	F12A—C11A—Cu	113.7 (13)
C2—C1—S2	124.3 (3)	F13A—C11A—Cu	114.8 (11)
S1—C1—S2	115.3 (2)	F11B—C11B—F12B	105.4 (14)
C1—C2—S3	120.4 (3)	F11B—C11B—F13B	104.8 (13)
C1—C2—S4	124.4 (3)	F11B—C11B—Cu	115.2 (13)
S3—C2—S4	115.2 (2)	F12B—C11B—F13B	101.5 (14)
C4—C3—S1	116.7 (3)	F12B—C11B—Cu	112.6 (11)
C4—C3—S5	128.7 (3)	F13B—C11B—Cu	115.9 (11)
S1—C3—S5	114.5 (2)	F21A—C12—F22A	115.4 (7)
C3—C4—S2	117.4 (3)	F21A—C12—F23A	103.7 (6)
C3—C4—S6	129.0 (3)	F21A—C12—Cu	116.7 (5)
S2—C4—S6	113.6 (2)	F22A—C12—F23A	98.3 (5)
C6—C5—S3	117.1 (3)	F22A—C12—Cu	113.2 (5)
C6—C5—S7	129.3 (3)	F23A—C12—Cu	106.8 (4)
S3—C5—S7	113.6 (2)	F21B—C12—F22B	108.9 (6)
C5—C6—S4	117.3 (3)	F21B—C12—F23B	94.5 (5)
C5—C6—S8	128.0 (3)	F21B—C12—Cu	116.0 (4)
S4—C6—S8	114.7 (2)	F22B—C12—F23B	100.0 (6)
C8—C7—S5	113.8 (3)	F22B—C12—Cu	122.7 (5)
C7—C8—S6	114.8 (3)	F23B—C12—Cu	109.6 (4)
C10—C9—S7	113.7 (3)	C14—C13—Cl1	110.0 (6)
C9—C10—S8	113.8 (3)	C14—C13—Cl2^i	104.2 (5)
C11A—Cu—C12	96.4 (5)	Cl1—C13—Cl2^i	115.0 (4)
C11A—Cu—C11B^i	89.1 (5)	C13—C14—Cl2	104.3 (5)

Symmetry code: (i) $x, \frac{1}{2} - y, z$.

Table 4. *Geometric parameters* (Å, °) *in* κ_L-(ET)$_2$Ag(CF$_3$)$_4$(TCE)

S1—C1	1.742 (4)	C9—C10	1.513 (8)
S1—C3	1.746 (5)	Ag—C11A	2.09 (4)
S2—C1	1.746 (5)	Ag—C11B	2.11 (4)
S2—C4	1.761 (5)	Ag—C12	2.094 (5)
S3—C2	1.745 (5)	C11A—F11A	1.25 (4)
S3—C5	1.752 (4)	C11A—F12A	1.29 (3)
S4—C2	1.742 (4)	C11A—F13A	1.30 (3)
S4—C6	1.751 (5)	C11B—F11B	1.41 (3)
S5—C3	1.753 (4)	C11B—F12B	1.33 (4)
S5—C7	1.807 (5)	C11B—F13B	1.30 (2)
S6—C4	1.748 (5)	C12—F21A	1.307 (9)
S6—C8	1.816 (5)	C12—F22A	1.294 (13)
S7—C5	1.742 (4)	C12—F23A	1.396 (9)
S7—C9	1.808 (5)	C12—F21B	1.322 (9)
S8—C6	1.753 (5)	C12—F22B	1.314 (12)
S8—C10	1.808 (5)	C12—F23B	1.404 (9)
C1—C2	1.361 (6)	C13—C14	1.491 (13)
C3—C4	1.350 (6)	C13—Cl1	1.821 (9)
C5—C6	1.345 (6)	C13—Cl2^i	1.912 (9)
C7—C8	1.517 (7)	C14—Cl2	1.760 (9)
C1—S1—C3	95.7 (2)	C11A—Ag—C12^i	173.0 (5)
C1—S2—C4	95.0 (2)	C11B—Ag—C12	87.3 (9)
C2—S3—C5	95.0 (2)	C11B—Ag—C12^i	174.8 (5)
C2—S4—C6	94.9 (2)	C12—Ag—C12^i	89.1 (3)
C3—S5—C7	99.9 (2)	F11A—C11A—F12A	107 (3)
C4—S6—C8	101.9 (2)	F11A—C11A—F13A	101 (2)
C5—S7—C9	101.1 (2)	F11A—C11A—Ag	116 (3)
C6—S8—C10	100.9 (2)	F12A—C11A—F13A	104 (3)
C2—C1—S1	120.5 (3)	F12A—C11A—Ag	114 (2)
C2—C1—S2	124.4 (3)	F13A—C11A—Ag	114 (2)
S1—C1—S2	115.1 (2)	F11B—C11B—F12B	104 (2)
C1—C2—S3	120.4 (3)	F11B—C11B—F13B	102 (3)
C1—C2—S4	124.3 (3)	F11B—C11B—Ag	111 (2)
S3—C2—S4	115.2 (2)	F12B—C11B—F13B	104 (2)
C4—C3—S1	116.9 (3)	F12B—C11B—Ag	116 (2)
C4—C3—S5	128.4 (4)	F13B—C11B—Ag	118 (2)
S1—C3—S5	114.7 (3)	F21A—C12—F22A	110.4 (10)
C3—C4—S2	117.2 (3)	F21A—C12—F23A	102.8 (8)
C3—C4—S6	129.1 (4)	F21A—C12—Ag	114.1 (5)
S2—C4—S6	113.7 (3)	F22A—C12—F23A	101.6 (7)
C6—C5—S3	116.9 (3)	F22A—C12—Ag	114.2 (7)
C6—C5—S7	129.5 (4)	F23A—C12—Ag	112.4 (5)
S3—C5—S7	113.5 (2)	F21B—C12—F22B	106.4 (9)
C5—C6—S4	117.4 (3)	F21B—C12—F23B	100.2 (7)
C5—C6—S8	127.9 (4)	F21B—C12—Ag	116.3 (5)
S4—C6—S8	114.7 (3)	F22B—C12—F23B	100.8 (8)
C8—C7—S5	113.4 (3)	F22B—C12—Ag	118.2 (6)
C7—C8—S6	115.1 (3)	F23B—C12—Ag	112.5 (4)
C10—C9—S7	113.4 (4)	C14—C13—Cl1	110.0 (6)
C9—C10—S8	113.4 (4)	C14—C13—Cl2^i	104.5 (6)
C11A—Ag—C12	94.2 (9)	Cl1—C13—Cl2^i	113.8 (5)
C11A—Ag—C11B^i	89.9 (4)	C13—C14—Cl2	104.8 (6)

Symmetry code: (i) $x, \frac{1}{2} - y, z$.

state because of the bonding and antibonding character, respectively, of the highest occupied molecular orbitals (Mori, Kobayashi, Sasaki, Kobayashi, Saito & Inokuchi, 1984). In practice, low-temperature structural studies are necessary in order to achieve sufficient accuracy from the X-ray diffraction experiment. The bonds between the S atoms and the outer ethylene group C atoms are slightly longer, averaging 1.81 Å, since these bonds are not part of the π-conjugated system. The ethylene groups in both salts are ordered and deviate noticeably from the molecular plane. In the present structures, they adopt an eclipsed conformation, *i.e.* when viewed along the long molecular axis, the two ethylene group C—C bonds are

on top of each other in their twist out of the molecular plane. The eclipsed conformation is found in most of the κ-phase ET-based superconductors.

The packing of the ET molecules within the *ac* plane (shown in Fig. 3) follows closely that of the other κ-phase ET salts, *e.g.* κ-(ET)$_2$Cu[N(CN)$_2$]Br. The hallmark of the κ-phase packing pattern is the presence of parallel dimers, usually with a center of inversion in the middle, although exceptions occur, *viz.* κ-(ET)$_2$Cu(NCS)$_2$ (a noncentrosymmetric structure, where the two molecules forming a dimer are not crystallographically equivalent, although within the donor molecule layer, the deviations from centro-

symmetry are slight; Urayama, Yamochi, Saito, Sato, Kawamoto, Tanaka, Mori, Maruyama & Inokuchi, 1988). When projected onto the plane of the ET molecules, the two molecules are displaced by *ca* 1.5 Å along the C=C bond direction, leading to a 'bond-over-ring' arrangement, as is the case in most of the superconducting κ-phase salts (Jung, Evain, Novoa, Whangbo, Beno, Kini, Schultz, Williams & Nigrey, 1989). This arrangement minimizes repulsive intermolecular interactions within the dimer, while keeping the packing as compact as possible. The only intermolecular contacts shorter than the sum of the van der Waals radii (Bondi, 1964) involve one of the H atoms bound to C9 (see Table 5).

The molecular plane of the ET molecules is inclined *ca* 45° with respect to the *c* axis. By application of a
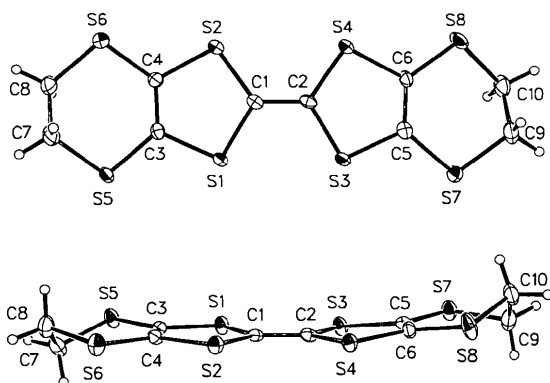
Fig. 2. Top and side view of the ET molecule in κ*L*-(ET)2Cu(CF3)4(TCE), with atomic labels. The molecular conformation and the thermal ellipsoids (here drawn at the 50% probability level, except for the H atoms which are drawn with an arbitrary circle radius) are virtually indistinguishable from those in κ*L*-(ET)2Ag(CF3)4(TCE).

Table 5. *Intermolecular contacts shorter than the sum of the corresponding van der Waals radii* (Å)

S: 1.80, Cl: 1.75, C: 1.70, F: 1.47, H: 1.20 Å (Bondi, 1964).

	Cu salt	Ag salt	Σr_{vdW}
S1···S7^i	3.563 (2)	3.578 (2)	3.60
S4···S7^{ii}	3.541 (2)	3.541 (2)	3.60
S5···S7^i	3.484 (2)	3.498 (2)	3.60
S8···F13B^{iii}	3.088 (6)	3.159 (8)	3.27
S8···Cl2^{iv}	3.472 (2)	3.482 (2)	3.55
C7···F21A^v	3.106 (8)	3.097 (9)	3.17
C7···F21B^v	3.161 (8)	3.146 (9)	3.17
C9···F11A^i	2.986 (13)	3.026 (16)	3.17
C9···F21B^i	3.040 (8)	3.041 (9)	3.17
C10···F11A^i	2.928 (14)	3.019 (16)	3.17
C10···F23A^{iii}	3.092 (8)	3.239 (11)	3.17
H7A···H9B^{iv}	2.401/2.196*	2.415/2.212	2.40
H7A···F21A^v	2.494/2.423 (7)	2.527/2.465 (9)	2.67
H7A···F21B^v	2.409/2.311 (6)	2.407/2.312 (7)	2.67
H7B···F12A	2.540/2.423 (11)	2.469/2.352 (14)	2.67
H7B···F12B	2.709/2.586 (10)	2.670/2.553 (12)	2.67
H8A···S8^{vi}	2.778/2.656 (1)	2.812/2.690 (2)	3.00
H9A···F11A^i	2.283/2.195 (14)	2.293/2.197 (16)	2.67
H9A···F21B^i	2.600/2.559 (7)	2.568/2.522 (8)	2.67
H9A···F11B^i	2.678/2.585 (12)	2.802/2.716 (15)	2.67
H9A···F13B^i	2.722/2.586 (6)	2.658/2.521 (8)	2.67
H9A···F23A^i	2.848/2.753 (7)	2.732/2.647 (9)	2.67
H9B···S6^{iv}	2.899/2.786 (1)	2.912/2.799 (1)	3.00
H9B···C4^{iv}	2.915/2.796 (4)	2.898/2.777 (5)	2.90
H10A···F11A^i	2.464/2.419 (13)	2.623/2.589 (16)	2.67
H10A···F21B^i	2.662/2.585 (8)	2.724/2.653 (11)	2.67
H10B···F23A^{iii}	2.577/2.522 (6)	2.641/2.574 (8)	2.67
H10B···F22B^{iii}	2.755/2.688 (8)	2.692/2.628 (12)	2.67
H13···F23B^{vii}	2.481/2.373 (6)	2.610/2.502 (9)	2.67
H13···F23B^v	2.602/2.480 (6)	2.726/2.626 (9)	2.67
H13···F21A^{vii}	2.715/2.662 (9)	2.577/2.506 (10)	2.67
H14A···F12B^{viii}	2.272/2.150 (12)	2.441/2.321 (15)	2.67
H14A···F12A^{viii}	2.562/2.460 (11)	2.565/2.463 (18)	2.67
H14A···F12B^{ix}	2.630/2.508 (11)	2.761/2.660 (15)	2.67
H14B···F13A	2.238/2.157 (6)	2.292/2.199 (11)	2.67
H14B···F13A^x	2.394/2.299 (6)	2.489/2.398 (11)	2.67
H14B···F22A^{xi}	2.552/2.459 (9)	2.552/2.472 (11)	2.67

Symmetry codes: (i) $1 - x, -y, 1 - z$; (ii) $-\frac{1}{2} + x, y, \frac{1}{2} - z$; (iii) $\frac{1}{2} - x, -y, -\frac{1}{2} + z$; (iv) $1 - x, -y, -z$; (v) $x, y, -1 + z$; (vi) $\frac{1}{2} - x, -y, \frac{1}{2} + z$; (vii) $x, \frac{1}{2} - y, -1 + z$; (viii) $\frac{1}{2} + x, y, \frac{1}{2} - z$; (ix) $\frac{1}{2} + x, \frac{1}{2} - y, \frac{1}{2} - z$; (x) $x, \frac{1}{2} - y, z$; (xi) $\frac{1}{2} + x, y, \frac{3}{2} - z$.

* For distances involving H atoms, the first value was calculated from the positions at $d_{C-H} = 0.95$ Å, and the second for $d_{C-H} = 1.09$ Å. The e.s.d.'s only include errors from the non-H atoms and lattice parameters.

Fig. 3. The packing of the ET molecules in the conducting layer of κ*L*-(ET)2Cu(CF3)4(TCE), as seen in a perspective projection along the long molecular axis of the ET molecule. Intermolecular S···S contacts shorter than 3.6 Å are indicated by thin lines.

twofold screw rotation parallel to the *c* axis, adjacent dimers are rotated by approximately 90° with respect to each other, giving the layer the appearance of a parquet tile pattern. The long axes of all molecules (*i.e.* the direction of the central C=C bond) within each plane are approximately parallel and lie roughly within the *ab* plane. However, they are inclined against the *b* axis by *ca* 36°, as seen in Fig. 1. Intermolecular S···S contacts shorter than the sum of the van der Waals radii (listed in Table 5) connect ET molecules belonging to different dimers. The contacts within each dimer are slightly longer. Short intermolecular S···S contacts are indicative of orbital overlap and thus electronic conduction pathways, although the cut-off criterion at the sum of the van der Waals radii is somewhat arbitrary due to the anisotropic extent of the sulfur π-orbitals. The two-dimensional topology of the S···S contacts is very

similar to that found in κ-(ET)$_2$Cu(NCS)$_2$, thus, similar electronic properties may be expected.

Subsequent cation radical layers are separated by the anions and the solvent molecules. A mirror plane is located at $y = 0.25$. Consequently, the tilt of the molecular axes against the b axis changes direction from one ET layer to the next, as seen in Fig. 1. The known κ-phase superconductors fall into two categories: one- and two-layer systems. The differences have been discussed in Williams, Ferraro, Thorn, Carlson, Geiser, Wang, Kini & Whangbo (1992). The title compounds are two-layer systems like κ-(ET)$_2$Cu[N(CN)$_2$]X ($X = $ Cl, Br, I), with whom they share the common space group $Pnma$ and gross unit-cell dimensions.

The major difference between the title compounds and the dicyanamide salts lies in the much increased spacing between adjacent ET molecular layers in the former. From center-to-center, this spacing is given by half the b unit-cell parameter, which is of the order 30 Å in the dicyanamide salts (at 127 K, $b = 29.658$, 29.681 and 30.050 Å for the Cl, Br and I salts, respectively). All the anion atoms of these salts are located on the mirror plane at $y = 0.25$, and one of the ET H atoms was in close contact with its mirror-symmetric equivalent across the mirror plane via an opening in the anion layer. In contrast, in the title compounds the b axes are 37.899 and 37.976 Å for the Cu- and Ag-containing salts, respectively. Thus, the conducting layers are almost 4 Å further separated than in the dicyanamide salts. It is expected that this increase in the layer spacing will manifest itself in more markedly two-dimensional physical properties, such as a higher anisotropy in the normal-state electrical conductivity. No crystals thick enough for conductivity measurements perpendicular to the layers have been obtained to date. The cause of the increased interlayer spacing is the manner in which the anions pack in the crystal structure.

The room-temperature structure of the PPN$^+$ [bis(triphenylphosphoranylidene)ammonium] salt of Cu(CF$_3$)$_4^-$ was reported by Naumann, Roy, Tebbe & Crump (1993). Unconstrained by symmetry requirements, the CuC$_4$-core of the complex anion was found to be almost planar with a slight tetrahedral distortion ($trans$-C—Cu—C angles: 165 and 172°). Under inclusion of the essentially ordered F atoms, the molecular symmetry of the anion in the PPN$^+$ salt was found to be approximately D_{2d}, with the trifluoromethyl groups lying on the apparent mirror planes. It was, therefore, a surprise to find that the crystallographic mirror plane in the κ_L-(ET)$_2$Cu(CF$_3$)$_4$(TCE) salt bisected the C—Cu—C angles rather than passing through one of the molecular mirror planes. Steric constraints require that adjacent CF$_3$ groups cannot be related by mirror symmetry, and therefore the anion must be disordered in the space group $Pnma$. It was possible to resolve the partially occupied atomic positions of the disordered model, and the result is shown in Figs. 4 and 5.

The anion in κ_L-(ET)$_2$Cu(CF$_3$)$_4$(TCE), as described by the resolved model, contains again a slightly tetrahedrally distorted square-planar CuC$_4$ core and trifluoromethyl groups whose orientation is rotated by approximately 180° upon proceeding from one group to the next. As in the PPN$^+$ salt, in each of the CF$_3$ groups, one of the F atoms, in projection along the Cu—C bond,
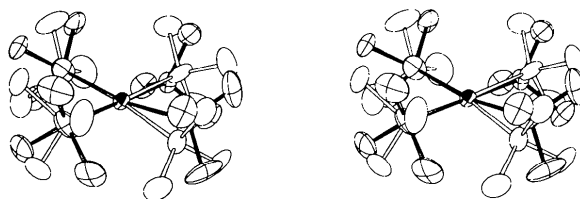

Fig. 4. Stereoview of the disordered anion in κ_L-(ET)$_2$Cu(CF$_3$)$_4$(TCE). One of the conformations is drawn with dark bonds and decorated ellipsoids, whereas the other mirror-symmetric conformation is drawn with open bonds and atomic ellipsoids.
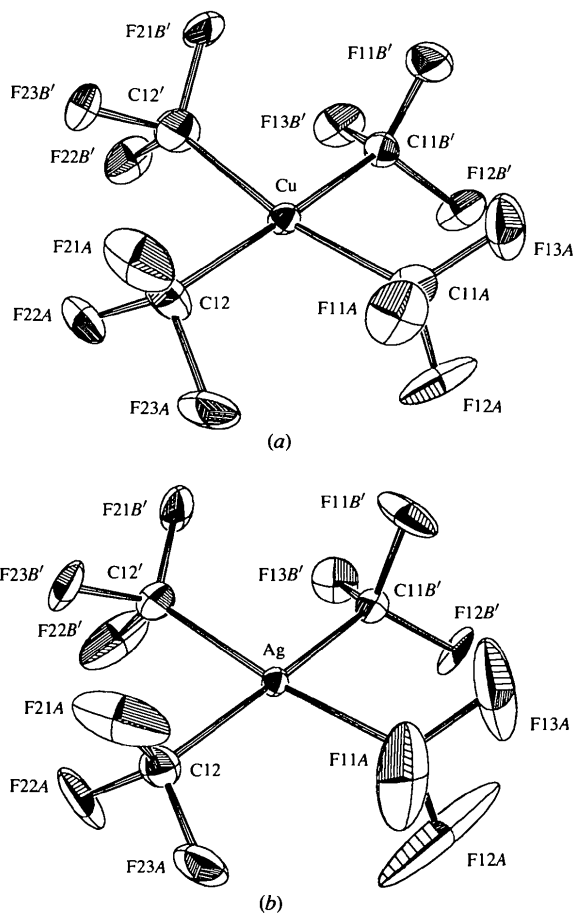

(a)

(b)

Fig. 5. The anions with atomic labels in (a) κ_L-(ET)$_2$Cu(CF$_3$)$_4$(TCE) and (b) κ_L-(ET)$_2$Ag(CF$_3$)$_4$(TCE). Only one molecular conformation is shown, and the thermal ellipsoids are drawn at the 50% probability level.

is parallel to the molecular pseudofourfold axis, whereas the other two F atoms are much closer to the molecular plane. The bond distances and angles, including the trans-C—Cu—C angles which quantify the tetrahedral distortion, are quite similar to those in the PPN⁺ salt. The scatter in C—F bond distances is probably due to high correlations among the coordinates of atoms belonging to the two disordered conformers.

The Ag(CF₃)₄⁻ anion is similar to the copper analog, except that the metal-to-carbon bonds are longer by ca 0.13 Å, and the trans-C—Ag—C angles are larger by ca 3–4°. Thus, the core of the silver complex is more closely square planar than the copper complex. Since the electronic structure of Cu^{3+} and Ag^{3+} are expected to be similar and favoring square-planar geometry, it is conjectured that the observed tetrahedral distortion is due to steric crowding of the F atoms between adjacent CF_3 groups. The increased bond length to the central metal atom decreases the crowding, and therefore, the Ag-containing complex is more planar. Furthermore, the F-atom thermal parameters in the Ag complex are larger than in its Cu counterpart, also indicating a less constricting environment for the trifluoromethyl groups, thereby allowing them to rotate at least partially.

The 1,1,2-trichloroethane solvent molecule was also found to be disordered across the mirror plane in both salts, see Fig. 6. The chlorine positions (one on the mirror plane and the other on a general position, thereby forming an isosceles triangle) were found to be common to both conformations of the molecule, at least within the resolution of the experiment. Any deviation from an exact superposition is likely absorbed into the thermal parameters. The C-atom positions belonging to each conformer were found on opposite sides of the mirror plane, since the C13—C14 distance between atoms on the same side of the mirror plane is too short for a C—C
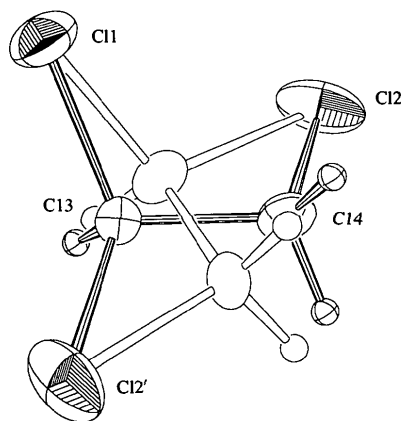
single bond. As seen in Fig. 6 and Tables 3 and 4, Cl2 is bound to C14 in one of the conformations, but to C13 in the other. The difference in the Cl2—C13 and Cl2—C14 bond lengths likely reflects that the superposition of the Cl2 sites for the two conformers is not entirely exact.

Fig. 7 shows a portion of the combined anion and solvent layer. Numerous short contacts (see Table 5) exist between the solvent molecule H atoms and the anion F atoms, suggesting hydrogen bonding. The packing of the layer is fairly efficient and without large holes. Any potential substitution of the TCE molecule by another solvent would require preservation of the overall shape, size and H-atom placement in order to allow for an isomorphous replacement, and thus preserve the superconducting properties. Of course, this observation does not preclude superconductivity in salts with different unrelated packing patterns. Weak hydrogen bonding also exists between the ethylene end groups of the ET molecules and the F atoms of the anion (see Table 5).

4. Concluding remarks

The crystal structures of κ_L-(ET)₂Cu(CF₃)₄(TCE) and κ_L-(ET)₂Ag(CF₃)₄(TCE) are virtually the same at 115–118 K. The limited experimental evidence available indicates that this is also the case at room temperature. The slight differences are due to the increase in the metal–carbon bond length of the anion by 0.13 Å upon replacing Cu by Ag. One of the effects is an increase in the unit-cell parameters by 0.14, 0.20 and 0.46% for the a, b and c axes, respectively. The relative increase is largest in the c direction, because the anion molecular plane is approximately parallel to the bc plane (see Fig.
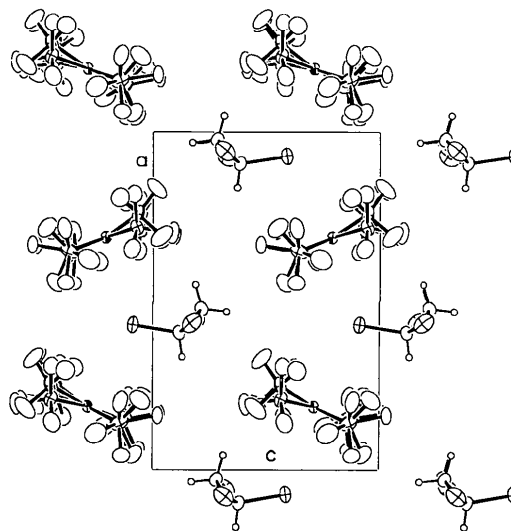

Fig. 6. The 1,1,2-trichloroethane solvent molecule with atomic labels in κ_L-(ET)₂Cu(CF₃)₄(TCE). Both mirror-symmetric conformations are shown in different drawing styles. The thermal ellipsoids are drawn at the 50% probability level.

Fig. 7. Molecular packing in the combined anion and solvent layer (ac plane near y = 0.25). The disordered components are drawn superimposed onto each other.

7), and the c axis is the shortest of the three. Within the anion, the longer metal–carbon bond leads to reduced steric crowding of the trifluoromethyl groups, which consequently exhibit larger thermal parameters in the silver-containing salt. Furthermore, the AgC_4 core is more planar than the CuC_4 entity, indicating that the electronic structure favors the planar configuration, but the steric crowding leads to a small tetrahedral distortion which is more pronounced in the copper case.

The κ-phase packing motif of the ET electron-donor molecules has yielded the organic superconductors with the highest values of T_c (excluding fullerides). The present compounds exhibit T_c's of less than half those found in κ-$(ET)_2Cu(SCN)_2$, κ-$(ET)_2Cu[N(CN)_2]Br$ (3) and κ-$(ET)_2Cu[N(CN)_2]Cl$ (4). We, therefore, need to examine the factors that render the $M(CF_3)_4^-$ salts unique, especially with regard to the copper dicyanamide-containing compounds, which have the same overall unit-cell packing and space group as the title compounds. In closely related superconductors, T_c usually increases with increasing unit-cell volume, since the density of states at the Fermi level increases, whereas the conduction band width decreases [see Williams, Ferraro, Thorn, Carlson, Geiser, Wang, Kini & Whangbo (1992) for discussion and further references]. However, in these almost two-dimensional systems, both the a and c axes of (1) and (2) are longer than those in both (3) and (4), whereas from the T_c's one would expect smaller values. Furthermore, the changes in lattice constants between (1) and (2) are in the opposite direction than those indicated by the transition temperatures. The major difference between the title compounds and the high T_c salts (3) and (4) is the thickness in the anion layer. In the latter, all the anion atoms are confined to the mirror plane, whereas in (1) and (2) the anion/solvent layer has substantial extent in the third dimension. This increased spacing between the conducting layers could lead to decreased coupling between the layers, and the lower T_c values could be due to this increase. The more likely reason, however, is the presence of crystallographic disorder in the anion/solvent plane. As mentioned in the *Introduction*, such disorder frequently suppresses T_c, often to the point where superconductivity is not observed at all. If the disorder is the cause of the reduced T_c's in these salts, it even rationalizes the difference between the Cu and the Ag salt. Thermal motion (partial rotation around the metal–carbon bond) of the trifluoromethyl groups, which are coupled to the conducting ET molecular layer *via* hydrogen bonds, is more pronounced in (2) than in (1). It would be desirable, *e.g.* by suitable substitution of the solvent molecule, to obtain an ordered κ-phase salt of either the $Cu(CF_3)_4^-$ or the $Ag(CF_3)_4^-$ salt, and to test if it has the higher T_c value [perhaps even higher than the current record holders, (3) and (4), based on the slightly larger a and c unit-cell parameters in (1) and (2)] expected for an ordered structure.

References

BECHGAARD, K., CARNEIRO, K., OLSEN, M., RASMUSSEN, F. B. & JACOBSEN, C. S. (1981). *Phys. Rev. Lett.* **46**, 852–855.

BECHGAARD, K., CARNEIRO, K., RASMUSSEN, F. B., OLSEN, M., RINDORF, G., JACOBSEN, C. S., PEDERSEN, H. J. & SCOTT, J. C. (1981). *J. Am. Chem. Soc.* **103**, 2440–2442.

BONDI, A. (1964). *J. Phys. Chem.* **68**, 441–451.

GEISER, U., SCHULTZ, A. J., WANG, H. H., WATKINS, D. M., STUPKA, D. L., WILLIAMS, J. M., SCHIRBER, J. E., OVERMYER, D. L., JUNG, D., NOVOA, J. J. & WHANGBO, M.-H. (1991). *Physica C (Amsterdam)*, **174**, 475–486.

GUBSER, D. U., FULLER, W. W., POEHLER, T. O., STOKES, J., COWAN, D. O., LEE, M. & BLOCH, A. N. (1982). *Mol. Cryst. Liq. Cryst.* **79**, 225–234.

ISHIGURO, T. & YAMAJI, K. (1990). *Organic Superconductors*. Berlin, Heidelberg: Springer-Verlag.

JUNG, D., EVAIN, M., NOVOA, J. J., WHANGBO, M.-H., BENO, M. A., KINI, A. M., SCHULTZ, A. J., WILLIAMS, J. M. & NIGREY, P. J. (1989). *Inorg. Chem.* **28**, 4516–4522.

KINI, A. M., GEISER, U., WANG, H. H., CARLSON, K. D., WILLIAMS, J. M., KWOK, W. K., VANDERVOORT, K. G., THOMPSON, J. E., STUPKA, D. L., JUNG, D. & WHANGBO, M.-H. (1990). *Inorg. Chem.* **29**, 2555–2557.

MORI, T., KOBAYASHI, A., SASAKI, Y., KOBAYASHI, H., SAITO, G. & INOKUCHI, H. (1984). *Bull. Chem. Soc. Jpn*, **57**, 627–633.

NAUMANN, D., ROY, T., TEBBE, K.-F. & CRUMP, W. (1993). *Angew. Chem. Int. Ed. Engl.* **32**, 1482–1483.

POUGET, J. P., SHIRANE, G., BECHGAARD, K. & FABRE, J. M. (1983). *Phys. Rev. B*, **27**, 5203–5206.

SCHLUETER, J. A., CARLSON, K. D., GEISER, U., WANG, H. H., WILLIAMS, J. M., KWOK, W.-K., FENDRICH, J. A., WELP, U., KEANE, P. M., DUDEK, J. D., KOMOSA, A. S., NAUMANN, D., ROY, T., SCHIRBER, J. E., BAYLESS, W. R. & DODRILL, B (1994). *Physica C*, **233**, 379–386.

SCHLUETER, J. A., CARLSON, K. D., WILLIAMS, J. M., GEISER, U., WANG, H. H., WELP, U., KWOK, W.-K., FENDRICH, J. A., DUDEK, J. D., ACHENBACH, C. A., NAUMANN, D., ROY, T., SCHIRBER, J. E. & BAYLESS, W. R. (1994). *Physica C*, **230**, 378–384.

SCHLUETER, J. A., GEISER, U., WILLIAMS, J. M., WANG, H. H., KWOK, W.-K., FENDRICH, J. A., CARLSON, K. D., ACHENBACH, C. A., DUDEK, J. D., NAUMANN, D., ROY, T., SCHIRBER, J. E. & BAYLESS, W. R. (1994). *J. Chem. Soc. Chem. Commun.* pp. 1599–1600.

SCHULTZ, A. J., WANG, H. H., WILLIAMS, J. M. & FILHOL, A. (1986). *J. Am. Chem. Soc.* **108**, 7853–7855.

STROUSE, C. (1985). *UCLA Crystallographic Package*. Univ. of California, Los Angeles, USA.

URAYAMA, H., YAMOCHI, H., SAITO, G., SATO, S., KAWAMOTO, A., TANAKA, J., MORI, T., MARUYAMA, Y. & INOKUCHI, H. (1988). *Chem. Lett.* pp. 463–466.

WILLIAMS, J. M., FERRARO, J. R., THORN, R. J., CARLSON, K. D., GEISER, U., WANG, H. H., KINI, A. M. & WHANGBO, M.-H. (1992). *Organic Superconductors (Including Fullerenes): Synthesis, Structure, Properties and Theory*. New Jersey: Prentice Hall.

WILLIAMS, J. M., KINI, A. M., WANG, H. H., CARLSON, K. D., GEISER, U., MONTGOMERY, L. K., PYRKA, G. J., WATKINS, D. M., KOMMERS, J. M., BORYSCHUK, S. J., STRIEBY CROUCH, A. V., KWOK, W. K., SCHIRBER, J. E., OVERMYER, D. L., JUNG, D. & WHANGBO, M.-H. (1990). *Inorg. Chem.* **29**, 3262–3274.

WILLIAMS, J. M., WANG, H. H., EMGE, T. J., GEISER, U., BENO, M. A., LEUNG, P. C. W., CARLSON, K. D., THORN, R. J., SCHULTZ, A. J. & WHANGBO, M.-H. (1987). *Progress in Inorganic Chemistry*, edited by S. J. LIPPARD, Vol. 35, pp. 51–218. New York: John Wiley & Sons, Inc.